Acta Mech 229, 4817–4830 (2018)
https://doi.org/10.1007/s00707-018-2261-9

ORIGINAL PAPER

I. P. Pegios · G. D. Hatzigeorgiou

Finite element free and forced vibration analysis of gradient elastic beam structures

Received: 22 February 2018 / Revised: 4 July 2018 / Published online: 27 September 2018

Abstract The dynamic stiffness matrix of a gradient elastic flexural Bernoulli–Euler beam finite element is analytically constructed with the aid of the basic and governing equations of motion in the frequency domain. The simple gradient theory of elasticity is used with just one material constant (internal length) in addition to the classical moduli. The flexural element has one node at every end with three degrees of freedom per node, i.e., the displacement, the slope, and the curvature. Use of this dynamic stiffness matrix for a plane system of beams enables one by a finite element analysis to determine its dynamic response harmonically varying with time external load or the natural frequencies and modal shapes of that system. The response to transient loading is obtained with the aid of Laplace transform with respect to time. A stiffness matrix is constructed in the transformed domain, the problem is formulated and solved by the finite element method, and the time domain response is finally obtained by a time domain inversion of the transform solution. Because the exact solution of the governing equation of motion in the frequency domain is used as the displacement function, the resulting dynamic stiffness matrices and the obtained structural response or natural frequencies and modal shapes are also exact. Examples are presented to illustrate the method and demonstrate its advantages. The effects of the microstructure on the dynamic behavior of beam structures are also determined.

1 Introduction

Micro-electro-mechanical systems (MEMS) and nano-electro-mechanical systems (NEMS) are usually modeled by linear elastic bars, beams, plates, and shells (Craighead [1]; Senturia [2]). Because of their extremely small dimensions, the behavior of these structures is significantly affected by their microstructure. Microstructural effects cannot be taken into account by the classical theory of elasticity, and one should use generalized or higher-order elasticity theories. These theories are characterized by non-locality of stress and internal length parameters and can take into account microstructural effects in a macroscopic manner.

Among those theories, Mindlin's [3] general theory of elasticity with microstructure, and in particular his form II theory associated with the second gradient of strain and consisting of just one constant (internal length) in addition to the other two classical elastic constants, has found many applications in structural analysis of microstructures. This simple theory, usually known as the gradient theory of elasticity, has been successfully used during the last 15 years or so to solve a variety of static and dynamic problems by analytical and numerical methods, as described, e.g., in the review article of Tsinopoulos et al. [4].

Most of the works on static and dynamic analysis of gradient elastic structures have been developed for beams. One can mention here the work of Chang and Gao [5], Papargyri-Beskou et al. [6,7], Lam et al. [8], Giannakopoulos and Stamoulis [9], Kong et al. [10], and Papargyri-Beskou and Beskos [11] on gradient elastic Bernoulli–Euler beams, and Papargyri-Beskou et al. [12], Wang et al. [13], Akgoz and Civalek [14],

I. P. Pegios · G. D. Hatzigeorgiou (✉)
School of Science and Technology, Hellenic Open University, 26335 Patras, Greece
E-mail: hatzigeorgiou@eap.gr

and Triantafyllou and Giannakopoulos [15] on gradient elastic Timoshenko beams. In all, of these works, the analysis was done by analytic methods and the beams were simple, statically determinate and under simple type of loading.

Problems of static and dynamic analysis of gradient elastic beams and beam structures involving statical indeterminacy, complex type of loading, and variable beam cross sections cannot be practically solved by analytical methods. Only numerical methods of solution, such as the finite element method (FEM), e.g., Martin [16], can be efficiently used for the above type of problems. Artan and Batra [17] and Artan and Toksoz [18] employed the method of initial values (also known as the matrix transfer method) to determine the eigenfrequencies and buckling loads, respectively, of simple gradient elastic Bernoulli–Euler beams under various boundary conditions at their two ends. The above method, even though it can be used for the solution of more complicated problems, such as those involving static indeterminacy and more than one beam members, is very complicated and inefficient in comparison with the FEM and for this reason its practical use is very limited.

Pegios et al. [19] have recently developed an FEM for the static and stability analysis of gradient elastic beams and beam structures by analytically constructing exact element stiffness matrices on the basis of displacement functions, which are the exact solution of the governing equations of the static and stability problems described in Papargyri-Beskou et al. [6]. Because exact stiffness matrices are used, the structural response is also exact, and one can model every beam member by only one finite element. Asiminas and Koumousis [20] have recently constructed stiffness and consistent mass matrices for Bernoulli–Euler beam elements on the basis of the gradient elastic theory of Papargyri-Beskou et al. [6] to study static and free vibration problems of simple beams. Their displacement function was a polynomial of the fifth degree with respect to the beam axis coordinate, and as a result of that their stiffness and mass matrices are approximate. Kahrobaiyan et al. [21] and Zhang et al. [22] have also recently constructed stiffness and consistent mass matrices for Bernoulli–Euler and Timoshenko beam elements, respectively, on the basis of the gradient elastic theory of Lam et al. [8]. The displacement function used by Kohrobaiyan et al. [21] is the exact solution of the governing equation of equilibrium, while that by Zhang et al. [22] the classical cubic polynomial. As a result of the above, Kohrobaiyan et al. [21] have exact stiffness and approximate mass matrices, while Zhang et al. [22] have approximate both stiffness and mass matrices. Approximate stiffness and/or mass matrices in FEM imply discretization of every member of the structure into 2–4 finite elements for acceptable accuracy. Finally, the similar works of Kahrobaiyan et al. [23] and Bakhtiari-Nejad et al. [24] can also be mentioned.

In this work, the dynamic stiffness matrix of a gradient elastic Bernoulli–Euler beam finite element is analytically/numerically constructed with the aid of the basic and governing equations of flexural motion of that element and its associated boundary conditions as described in Papargyri-Beskou et al. [7] in the frequency domain. Because the exact solution of the governing equation of motion in the frequency domain is used as the displacement function, the resulting dynamic stiffness matrices and hence the dynamic response to zero (free vibrations) or harmonically varying with time (forced vibrations) forces are the exact ones. When the external forces are general transient, the element dynamic stiffness is defined in the Laplace-transformed with respect to time domain. The problem is then formulated and solved in the transformed domain, and the time domain response is finally obtained by a numerical inversion of the transformed solution as described for classical beam structures in Beskos and Narayanan [25]. Thus, the present method is capable of providing the exact solution for both the free and forced vibration problems involving gradient elastic beams, in contrast to all the existing methods, which can only provide approximate solutions. Of course, the expressions for the coefficients of the dynamic stiffness matrices are more complicated here than in the other works. However, the discretization here involves only one finite element per physical member instead of 2–4 elements per physical member in all of the other methods.

Three examples are presented to illustrate the method and demonstrate its advantages. These examples deal with free and forced vibrations of statically determinate and indeterminate structures with loads harmonically varying with time and transient ones. In contrast, in all the existing works on the dynamics of gradient elastic beams, only examples involving free vibrations of simple statically determinate beams have been reported.

2 Gradient elastic beam theory

The basic and governing equations of a gradient elastic Bernoulli–Euler beam in bending under dynamic lateral loading as well as the associated classical and non-classical boundary conditions derived in Papargyri-Beskou et al. [7] are reproduced in this Section for reasons of completeness and easy reference.

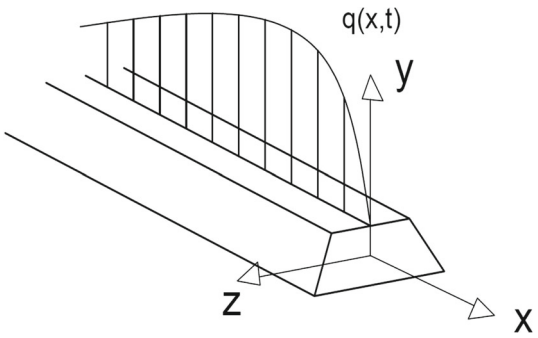

Fig. 1 Geometry and dynamic loading of a straight prismatic beam

Consider a straight prismatic beam under a dynamic lateral load $q(x,t)$ distributed along the longitudinal x axis of the beam, as shown in Fig. 1, where t denotes time. Thus, the loading plane is x–y, and the cross section A of the beam is characterized by the two axes y and z with the former one being its axis of symmetry. Under the lateral load $q(x,t)$, the beam experiences bending vibrations in the x–y plane measured by its lateral deflection $\upsilon(x,t)$ along the x axis. Axial deformation of the beam is considered to be negligible. Assuming gradient elastic material behavior, one has that the normal to the cross-sectional bending stress σ_x has the form

$$\sigma_x = E\left(\varepsilon_x - g^2\frac{\partial^2\varepsilon_x}{\partial x^2}\right) \tag{1}$$

where E is the modulus of elasticity, g is the gradient coefficient with dimensions of length (internal length representing the microstructural effects macroscopically), and ε_x is the normal bending strain expressed as

$$\varepsilon_x = -y\frac{\partial^2\upsilon}{\partial x^2}. \tag{2}$$

Using the deformation assumptions of the Bernoulli–Euler beam theory, the constitutive relation (1), the equilibrium of axial forces, and bending moments and the lateral inertia force, one can finally obtain the governing equation of lateral motion for the gradient elastic beam in terms of the lateral deflection $\upsilon(x,t)$ as in Papargyri-Beskou et al. [7],

$$\mathrm{EI}\left(\frac{\partial^4\upsilon}{\partial x^4} - g^2\frac{\partial^6\upsilon}{\partial x^6}\right) + \mu\frac{\partial^2\upsilon}{\partial t^2} = -q(x,t), \tag{3}$$

where I is the cross-sectional moment of inertia about the z axis and μ the mass per unit length of the beam. The above equation, which is of the sixth degree with respect to x, reduces to the classical one of the fourth degree for $g = 0$.

Assuming that the lateral load $q(x,t)$ varies harmonically with time in the form

$$q(x,t) = \overline{q}(x)e^{i\omega t}, \tag{4}$$

one has that the lateral deflection $\upsilon(x,t)$ also varies harmonically with time in the form

$$\upsilon(x,t) = v(x)e^{i\omega t} \tag{5}$$

where $\tilde{q}(x)$and $v(x)$ represent amplitudes, ω is the circular vibration frequency, and $i = \sqrt{-1}$. On account of Eqs. (4) and (5), Eq. (3) takes the form

$$v^{IV} - g^2 v^{VI} - \alpha^2 v = -\overline{q}/\mathrm{EI} \tag{6}$$

where primes and overdots indicate differentiation with respect to x and t, respectively, and

$$\alpha^2 = \frac{\mu\omega^2}{\mathrm{EI}}. \tag{7}$$

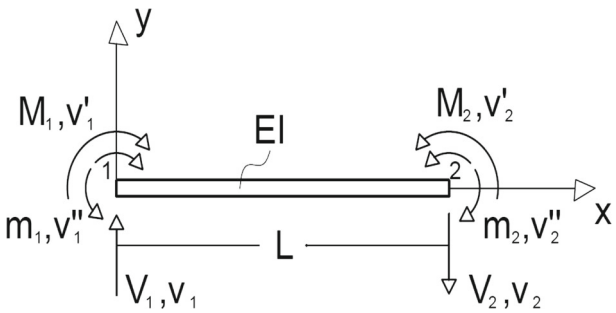

Fig. 2 Mechanics convention for generalized nodal forces and displacements of a gradient elastic flexural beam element in frequency domain

Equation (6) represents the governing equation of lateral motion of a gradient elastic beam in the frequency domain.

If one considers a beam element of length L with two ends defined by $x = 0$ and $x = L$, as shown in Fig. 2, and makes use of a variational statement, he can recover the governing equations (6) and all possible classical and non-classical boundary conditions so as to satisfy the following equations (Papargyri-Beskou et al. [7]):

$$\begin{aligned}
&\Big[V(L) - \mathrm{EI}[v'''(L) - g^2 v^V(L)]\Big]\delta v(L) - \Big[V(0) - \mathrm{EI}[v'''(0) - g^2 v^V(0)]\Big]\delta v(0) = 0,\\
&\Big[M(L) - \mathrm{EI}[v''(L) - g^2 v^{IV}(L)]\Big]\delta v'(L) - \Big[M(0) - \mathrm{EI}[v''(0) - g^2 v^{IV}(0)]\Big]\delta v'(0) = 0,\\
&\Big[[m(L) - EIg^2 v'''(L)]\Big]\delta v''(L) - \Big[[m(0) - EIg^2 v'''(0)]\Big]\delta v''(0) = 0.
\end{aligned} \tag{8}$$

In the above, V is the shear force, M is the bending moment, and m is the double moment due to the microstructure. This double moment m consists of two self-equilibrating moment vectors that do not contribute to the equilibrium equations but to the strain energy, as depicted in Fig. 2, where the positive directions of all forces and moments are also shown. It is observed that for $g = 0$ Eq. (8) reduces to the corresponding ones for the classical case.

If one assumes the four classical boundary conditions to be $v(0)$, $v(L)$, $v'(0)$ and $v'(L)$ prescribed and the non-classical ones to be $v''(0)$ and $v''(L)$ prescribed, then $\delta v(0) = \delta v(L) = 0$, $\delta v'(0) = \delta v'(L) = 0$, $\delta v''(0) = \delta v''(L) = 0$ and Eq. (8) are all satisfied. In view of Eq. (8) one can observe that, when dealing with the classical boundary conditions, either the deflections v or the shear forces $V = \mathrm{EI}(v'''(L) - g^2 v^V(L))$ and the strains (slopes) v' or the bending moments $M = \mathrm{EI}(v'' - g^2 v^{IV})$ at the boundaries (two ends) of the beam have to be specified. For the case of the non-classical boundary conditions, one has to specify either the boundary strain gradients (curvatures)v'' or the boundary double moments $m = EIg^2 v'''$.

3 Gradient elastic flexural dynamic stiffness matrix

This Section deals with the development of the dynamic stiffness matrix in the frequency domain of a gradient elastic flexural beam element with two nodes 1 and 2 at its two ends, as shown in Fig. 3. On the basis of Eq. (8) describing the boundary conditions of the problem, one concludes that there are three nodal generalized displacements (v, v', v'') and three nodal generalized forces (V, M, m) associated with those displacements at every node, as shown in Fig. 3. In other words, every node has three degrees of freedom (d.o.f.): displacement, slope, and curvature. These nodal generalized displacements and forces of Fig. 3 are considered to be positive. One can observe that the positive nodal quantities of Fig. 3 (matrix convention) are not the same as the corresponding ones of Fig. 2 (mechanics convention), and this fact has to be taken into account when transferring information from one Figure to the other.

For the construction of the stiffness matrix of the finite element of Fig. 3, one needs to select a displacement function and adopt a definition of that matrix. In this work, the displacement function is selected to be the exact solution of the homogeneous part of Eq. (6), which has the form

$$v(x, \omega) = \sum_{i=1}^{6} C_i e^{\lambda_i x} \tag{9}$$

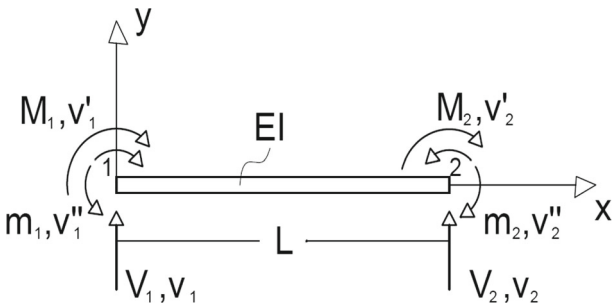

Fig. 3 Matrix convention for generalized nodal forces and displacements of a gradient elastic flexural beam element in frequency domain

where the, in general complex, exponents λ_i are the 6 roots of the algebraic equation

$$\lambda^4 - g^2\lambda^6 - \alpha^2 = 0 \tag{10}$$

which are functions of ω in view of relation (7) and C_i are the constants of integration to be determined. Because the exact solution of the governing equation of the problem is used as the displacement function, it is expected that the stiffness matrix to be constructed will be exact, and hence, the response of a beam structure to a mechanical loading analyzed on the basis of the FEM with that element stiffness matrix for every physical member will be also exact.

The dynamic stiffness matrix of the finite element of Fig. 3 will be constructed here on the basis of the displacement function (9) and the basic definition of any coefficient of that matrix. Thus, for the dynamic stiffness matrix $[k]$ connecting the vector of the amplitudes of the generalized nodal forces $\{f\}$ with the vector of the amplitudes of the corresponding nodal displacements $\{u\}$ as

$$\{f\} = [k]\{u\}, \tag{11}$$

the stiffness coefficient k_{ij} in the frequency domain is defined as the nodal generalized force at the degree of freedom i due to a unit nodal generalized displacement of the degree of freedom j, while all the other displacements are zero. It is obvious that since $v(x)$ depends on the frequency ω, so does the dynamic stiffness matrix $[k]$. In this work, since every node has 3 d.o.f., the finite element of Fig. 3 has $2 \times 3 = 6$ d.o.f., and hence, the size of the stiffness matrix $[k]$ will be 6×6, while the indices i, j will take the values 1,2,…,6. Thus, the dynamic stiffness matrix will be constructed here column by column on the basis of six generalized displacements states, the displacement function (9), and the expressions for V, M, m in terms of that displacement and its derivatives with respect to x as defined in Eq. (8).

Thus, the derivatives with respect to x of $v(x)$ of Eq. (9) are evaluated and listed as

$$v^{(n)}(x,\omega) = \sum_{i=1}^{6} C_i \lambda_i^n e^{\lambda_i x} \tag{12}$$

where the superscript (n) indicates the nth$(n = 1, 2, \ldots, 5)$ order derivative with respect to x, while the generalized forces V, M and m are expressed in terms of the above derivatives with the aid of Eq. (8) as

$$\begin{aligned} V(x,\omega) &= \mathrm{EI}[v'''(x,\omega) - g^2 v^V(x,\omega)], \\ M(x,\omega) &= \mathrm{EI}[v''(x,\omega) - g^2 v^{IV}(x,\omega)], \\ m(x,\omega) &= EIg^2 v'''(x,\omega). \end{aligned} \tag{13}$$

Consider the displacement state defined as

$$\begin{aligned} &v(0,\omega) = v_1 = 1, \quad v'(0,\omega) = v_1' = 0 \quad v''(0,\omega) = v_1'' = 0, \\ &v(L,\omega) = v_2 = 0, \quad v'(0,\omega) = v_2' = 0 \quad v''(0,\omega) = v_2'' = 0 \end{aligned} \tag{14}$$

where $v_1, v_1', v_1'', v_2, v_2', v_2''$ are the generalized nodal displacements of the finite element of Fig. 3. Equation (14), in view of the expressions (9) and (12), can be written in the form

$$\sum_{i=1}^{6} C_i = 1, \sum_{i=1}^{6} C_i \lambda_i = 0, \sum_{i=1}^{6} C_i \lambda_i^2 = 0,$$
$$\sum_{i=1}^{6} C_i e^{\lambda_i L} = 0, \sum_{i=1}^{6} C_i \lambda_i e^{\lambda_i L} = 0, \sum_{i=1}^{6} C_i \lambda_i^2 e^{\lambda_i L} = 0. \quad (15)$$

Equation (15) can be thought of as a linear system of six equations with six unknowns, the constants C_i $(i = 1, 2, \ldots, 6)$, which can be easily solved. Using the definition of the dynamic stiffness coefficients k_{ij} and the different sign convention of Fig. 2 (mechanics convention) and Fig. 3 (matrix convention), one can obtain the dynamic stiffness coefficients for the first column of $[k]$ corresponding to the displacement state (14) in the form

$$k_{11} = V(0, \omega), \quad k_{21} = M(0, \omega), \quad k_{31} = m(0, \omega),$$
$$k_{41} = -V(L, \omega), \quad k_{51} = -M(L, \omega), \quad k_{61} = -m(L, \omega), \quad (16)$$

where the right-hand sides of Eq. (16) can be computed by using Eqs. (13), (9), and (12) with values of the constants $C_i (i = 1, 2, \ldots, 6)$, those obtained from the solution of Eq. (15). Because Eq. (10) has to be solved analytically, the whole above-mentioned procedure for the computation of the k_{ij} of Eq. (16) is done analytically with the aid of Mathematica [26].

Considering the second displacement state

$$v(0, \omega) = v_1 = 0, \quad v'(0, \omega) = v_1' = 1 \quad v''(0, \omega) = v_1'' = 0,$$
$$v(L, \omega) = v_2 = 0, \quad v'(L, \omega) = v_2' = 0 \quad v''(L, \omega) = v_2'' = 0, \quad (17)$$

and following exactly the same procedure as before, one can obtain the dynamic stiffness coefficients of the second column of the matrix $[k]$ in the form

$$k_{12} = V(0, \omega), \quad k_{22} = M(0, \omega), \quad k_{32} = m(0, \omega),$$
$$k_{42} = -V(L, \omega), \quad k_{52} = -M(L, \omega), \quad k_{62} = -m(L, \omega). \quad (18)$$

After repeating the above procedure four more times, the remaining four columns of the matrix $[k]$ can be also determined. Due to the symmetry of the matrix $[k]$, the satisfaction of the relation $k_{ij} = k_{ji}$ with the aid of Mathematica [26] serves as a verification of the exactness of these expressions for k_{ij}. The vectors $\{f\}$ and $\{u\}$ connected through the dynamic stiffness matrix $[k]$ for the finite element of Fig. 3 are explicitly written down as

$$\{f\} = \{V_1, M_1, m_1, V_2, M_2, m_2\}^T,$$
$$\{u\} = \{v_1, v_1', v_1'', v_2, v_2', v_2''\}^T \quad (19)$$

while the various elements k_{ij} of the dynamic matrix $[k]$ determined with the aid of Mathematica [26] are not shown explicitly here due to their complexity.

4 Free and forced flexural vibrations

Consider a beam structure experiencing flexural vibrations under dynamic loading varying harmonically with time. Following standard procedures (e.g., Martin [16]), one is able to formulate this problem into a FEM form in the frequency domain reading as

$$\{F\} = [K(\omega)]\{U\}. \quad (20)$$

In the above, $[K(\omega)]$ is the total structural dynamic stiffness matrix depending on frequency ω and obtained as an appropriate superposition of the dynamic stiffness matrices $[k]$ of the various finite elements comprising the structure, and $\{U\}$ and $\{F\}$ are the vectors of the amplitudes of the generalized nodal displacements and

external forces of the whole structure, respectively. After application of the boundary conditions of the problem in terms of the generalized nodal displacements, one can solve Eq. (20) and determine the unknown amplitudes of the generalized nodal displacements in terms of the known operational frequency ω.

In case of free vibrations, one has $\{F\}$=$\{0\}$, and in order for the resulting equation in (20) after application of the boundary conditions to have nonzero solutions for $\{U\}$, the condition

$$Det[K(\omega)] = 0 \tag{21}$$

should be satisfied. Equation (21) is the frequency equation with roots $\omega_i (i = 1, 2, \ldots, \infty)$, the natural frequencies of the beam structure. Once the natural frequencies have been obtained, the modal shapes $\{U\}$ can be also determined from (20) with $\{F\}$=$\{0\}$ in the standard way. Because Eq. (21) is too complicated, it can only be solved numerically by determining the value of the $\det[K(\omega)]$ for a sequence of values of ω and recording those values for which (21) is satisfied. However, since the whole procedure involves complex arithmetics, one computes the real-valued function $D(\omega) = \ln|\det[K(\omega)]|$ for a sequence of values of ω and identifies the natural frequencies as the local minima of $D(\omega)$ by following Kitahara [27].

When the external loading is transient, the whole problem is solved in the Laplace transform with respect to the time domain, and the time domain response is obtained by a numerical inversion of the transformed solution (Beskos and Narayanan [25]). Consider the Laplace transform $\overline{\Phi}(x, s)$ defined for a function $\Phi(x, t)$ as

$$\overline{\Phi}(x, s) = \int_0^\infty \Phi(x, t) e^{-st} \mathrm{d}t \tag{22}$$

where s is the, in general complex, Laplace transform parameter. Application of the above Laplace transform onto Eq. (3) under zero initial conditions results in

$$\overline{v}^{IV} - g^2 \overline{v}^{VI} + \alpha^2 \overline{v} = -\overline{q}/\mathrm{EI} \tag{23}$$

where

$$\alpha^2 = \frac{\mu s^2}{\mathrm{EI}} \tag{24}$$

and indicates that one can go from the frequency into the Laplace transform domain by simply replacing ω by $-is$. Hence, Eq. (20) can also be used in the Laplace transform domain in the form

$$\{\overline{F}\} = [K(s)]\{\overline{U}\} \tag{25}$$

where $[K(s)]$ is the $[K(\omega)]$ with $\omega = -is$ and overbars in vectors $\{\overline{U}\}$and $\{\overline{F}\}$indicate transformed quantities. Equation (25) is solved numerically for $\{\overline{U}\}$ for a sequence of values of s, and the transformed solution is inverted numerically to obtain the time domain response. This inversion is done with the highly accurate algorithm of Durbin [28] as explained in Narayanan and Beskos [29].

5 Numerical examples

Three examples are presented in this Section to illustrate the use of the previously developed dynamic stiffness matrices in the framework of the FEM, demonstrate the advantages of the whole procedure for analyzing the dynamic behavior of gradient elastic beam structures, and assess the effects of the microstructure on that behavior. The first two examples deal with free and forced vibrations of two statically determinate structures (cantilever and simply supported beams), while the third example with free and forced vibrations of a statically indeterminate beam structure with non-uniform section.

Example 1 Consider a gradient elastic uniform cantilever beam of length L and flexural rigidity EI subjected to a vertical lateral concentrated load P_0 suddenly applied at its free end ($P(\mathrm{t}) = P_\mathrm{o}\mathrm{H(t)}$), as shown in Fig. 4. For this structure the first five natural frequencies and its dynamic response to the load $P(\mathrm{t})$ are determined by the FEM.

The whole beam is considered to be a single finite element with nodes 1 and 2 at the fixed and free ends, respectively, as shown in Fig. 4. The dynamic response of that beam element 1–2 to a load $P(t) = P_\mathrm{o}\mathrm{e}^{\mathrm{i}\omega t}$ is described by the stiffness equation (11) in the frequency domain with $[k]$ being of the order of 6×6. Application of the boundary conditions

$$v_1 = v_1' = v_1'' = 0 \tag{26}$$

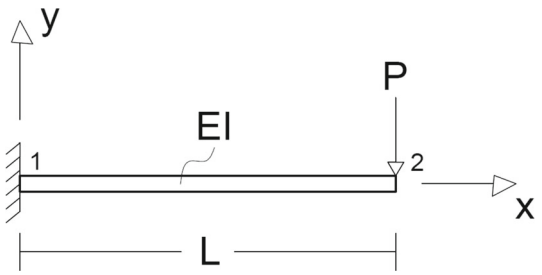

Fig. 4 Geometry and loading of a cantilever gradient elastic flexural beam

Table 1 First five normalized natural frequencies of a gradient elastic cantilever beam for various values of g/L

g/L	0.0001	0.005	0.010	0.050	0.100
1st	1.0000	1.01018	1.02037	1.10658	1.22523
2nd	1.0000	1.01028	1.02102	1.12476	1.29145
3rd	1.0000	1.01059	1.02258	1.16470	1.42304
4th	1.0000	1.01124	1.02525	1.22553	1.60883
5th	1.0000	1.01227	1.02903	1.30263	1.82896

with the first two conditions in (26) being the classical and the third condition the non-classical one, reduces Eq. (11) to the form

$$\begin{Bmatrix} -P_0 \\ 0 \\ 0 \end{Bmatrix} = \begin{vmatrix} k_{44} & k_{45} & k_{46} \\ k_{54} & k_{55} & k_{56} \\ k_{64} & k_{65} & k_{66} \end{vmatrix} \begin{Bmatrix} v_2 \\ v_2' \\ v_2'' \end{Bmatrix} \tag{27}$$

where $k_{ij} = k_{ij}(\omega)$ and P_0, v_2, v_2' and v_2'' stand for amplitudes. The frequency equation (21) with $[k(\omega)]$ being explicitly given in (27) is solved as described in Sect. 4, and the first five normalized natural frequencies $\omega_k/\omega_k^c (k = 1, 2, \ldots, 5)$ are shown in Table 1 for various values of the normalized gradient coefficient g/L. The normalizing factors $\omega_n^c (n = 1, 2, \ldots, 5)$ are the classical natural frequencies $\omega_n^c = [(2n-1)^2\pi^2/4L^2]\sqrt{\mathrm{EI}/\mu}$.

One can observe from Table 1 that the frequencies increase for increasing values of the gradient coefficient, which is expected due to the stiffening effect of gradient elasticity (e.g., Papargyri-Beskou et al. [7]). Furthermore, one can observe from Table 1 that for $g/L = 0.0001$ (practically zero) one recovers the values of the natural frequencies for the classical case.

The forced vibration problem is described by Eq. (27) considered to be in the Laplace-transformed domain. In that case P_0 is replaced by P_0/s, $k_{\mathrm{ij}}(\omega)$ become $k_{\mathrm{ij}}(s)$ by simply replacing ω by -is, and v_2, v_2' and v_2'' become $\overline{v}_2$, $\overline{v}_2'$ and $\overline{v}_2''$, respectively. Thus, according to Sect. 4, Eq. (27) in the Laplace-transformed domain is solved for a sequence of values of s, and the time domain response is obtained by a numerical inversion of the transformed solution using the algorithm of Durbin [28]. Figure 5 provides the free end deflection of the cantilever beam versus time for various values of g/L on the basis of the data in Papargyri-Beskou et al. [7] reading as L=1.219 m, $I = 5993.73\ \mathrm{cm}^4$, $E = 20.685 \times 10^4$ MPa, $\mu = 60.709$ kg/m, and $P_0 = 35584$ N. The present results are identical with those in Papargyri-Beskou et al. [7] obtained by an analytical method. One can observe from Fig. 5 that increasing values of g/L decrease the maximum values of the deflection and shift them to smaller time values of occurrence. Furthermore, one can observe that for $g = 0$ one can recover the response of the classical case (Beskos and Michael [30]), as expected.

Example 2 Consider a simply supported gradient elastic beam of length $2L$ and flexural rigidity EI under a lateral concentrated vertical dynamic load P(t) at the middle of its span, as shown in Fig. 6. The above beam is considered as a beam structure composed of two finite elements 1–2 and 2–3, as shown in Fig. 6. With 3 d.o.f. per node, the whole beam has $3 \times 3 = 9$ d.o.f., and hence, the total structural dynamic stiffness matrix $[K]$ will be of the order of 9×9. This dynamic stiffness matrix is obtained by a simple superposition of the stiffness matrices 6×6 of the finite elements 1–2 and 2–3 as given by Eq. (11) by following standard procedures (Martin [16]).

The classical boundary conditions of the problem in terms of generalized nodal displacements are

$$v_1 = v_3 = v_2' = 0 \tag{28}$$

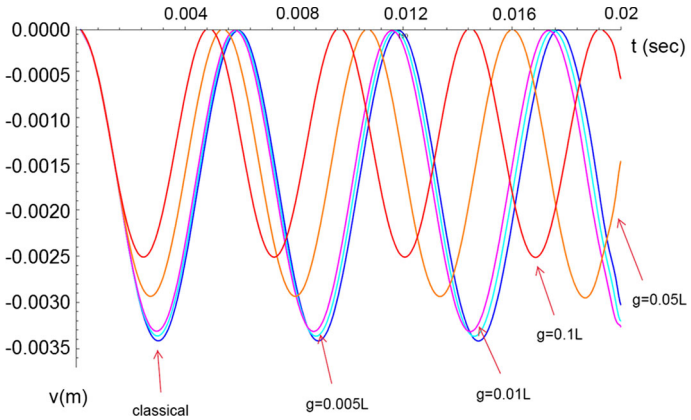

Fig. 5 Free end deflection of a gradient elastic cantilever beam versus time for various values of g/L (load $P = Po * H(t)$)

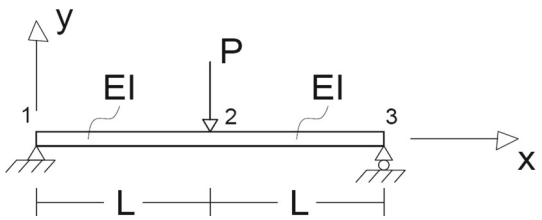

Fig. 6 Geometry and dynamic loading of a simply supported gradient elastic flexural beam

where the third boundary condition in (28) comes from symmetry considerations. The non-classical boundary conditions are assumed to be

$$v_1'' = v_3'' = 0. \tag{29}$$

Thus, the total structural dynamic stiffness matrix of order 9×9, due to the 5 boundary conditions (28) and (29), becomes 4×4, and the stiffness equation in the frequency domain takes the form (20) with

$$\begin{aligned} \{F\} &= \{0, -P_o, 0, 0\}^{\mathrm{T}}, \\ \{U\} &= \{v_1', v_2, v_2'', v_3'\}^{\mathrm{T}} \end{aligned} \tag{30}$$

where all the entries in the vectors of Eq. (30) denote amplitudes and $P(\mathrm{t}) = P_0 \sin\omega \mathrm{t}$. With known operational frequency ω and load amplitude P_0, one can solve Eq. (20) for $\{U\}$. Figure 7 depicts $v_2(\mathrm{t}) = v_2 \sin\omega \mathrm{t}$ versus t for $\omega = 1500\,\mathrm{rad/s}$ and various values of g/L. The geometry and material data are the same as in Example1. In the same Figure, the analytical solution as given in Rao [31], is also plotted for the classical case ($g = 0$) and shown to coincide with the FEM solution for $g/L = 0.0001$ (practically zero).

The same forced vibration problem was also solved by assuming the external load $P(t) = P_0 \sin\omega \mathrm{t}$ to be a transient one. In that case Eq. (25) is used with $\{\overline{F}\}$ and $\{\overline{U}\}$ given by

$$\begin{aligned} \{\overline{F}\} &= \{0, -\overline{P}, 0, 0\}^{\mathrm{T}}, \\ \{\overline{U}\} &= \{\overline{v}_1', \overline{v}_2, \overline{v}_2'', \overline{v}_3'\}^{\mathrm{T}} \end{aligned} \tag{31}$$

where $\overline{P} = P_0 \frac{\omega}{s^2+\omega^2}$. Equation (25) with $\{\overline{F}\}$ and $\{\overline{U}\}$ as in (31) was solved for a sequence of values of s, and the transformed solution $\overline{v}_2$ was numerically inverted with the aid of Durbin's [28] algorithm to provide the time domain solution $v_2(t)$. It was found that this solution was identical to the one depicted in Fig. 7.

Figure 8 shows the $v_2(\mathrm{t})$ versus time and various values of g/L for the case of the load being suddenly applied ($\mathrm{P(t)} = \mathrm{P_0 H(t)}$). The problem is solved in the Laplace domain, and the response is obtained by a numerical inversion of the transformed solution, as described previously. From Figs. 7 and 8 one can observe a decrease of the deflection for increasing values of g/L (stiffening effect of gradient elasticity).

For the simply supported beam of Fig. 6 the first five natural frequencies were also computed by solving Eq. (21) as described in Sect. 4. For this free vibration problem there is no need to consider the beam structure

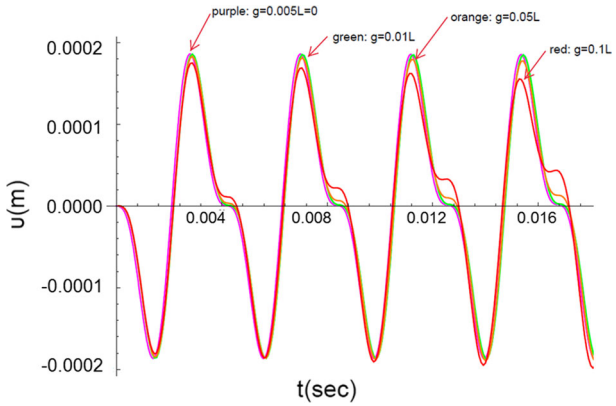

Fig. 7 Mid-span deflection of a gradient elastic simply supported beam versus time for various values of g/L (load $P(t) = Po * \sin\omega t$)

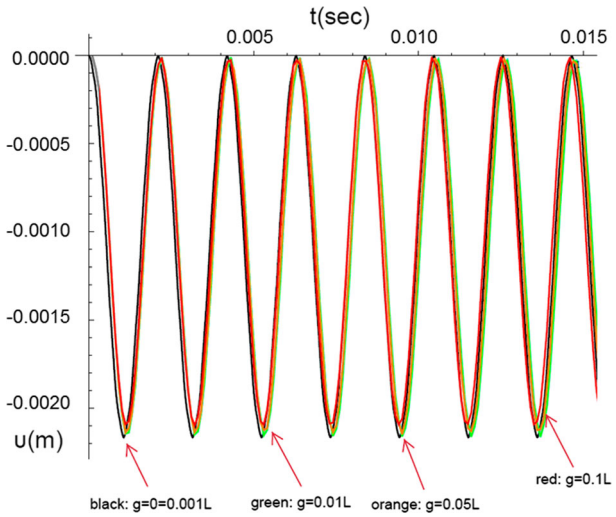

Fig. 8 Mid-span deflection of a gradient elastic simply supported beam versus time for various values of g/L (load $P(t) = Po * H(t)$)

as composed of two finite elements as in the case of forced vibrations. Considering one beam element for the beam 1–3 of Fig. 6 and boundary conditions

$$v_1 = v_1'' = v_3 = v_3'' = 0, \tag{32}$$

the dynamic stiffness matrix is of the order of 2×2, and Eq. (20) in the absence of external load (free vibrations) takes the form

$$\begin{bmatrix} D_{22} & D_{25} \\ D_{52} & D_{55} \end{bmatrix} \begin{Bmatrix} v_1' \\ v_3' \end{Bmatrix} = \begin{Bmatrix} 0 \\ 0 \end{Bmatrix}. \tag{33}$$

Thus, in view of (33), Eq. (21) takes the form

$$D_{22}D_{55} - D_{25}^2 = 0, \tag{34}$$

and since D_{ij} coefficients are functions of ω, the solution of Eq. (34) provides the natural frequencies of the beam.

Table 2 shows the normalized first five natural frequencies for various values of g/L with the normalizing factors ω_n^c being the classical natural frequencies $\omega_n^c = (n^2\pi^2/4L^2)\sqrt{\mathrm{EI}/\mu}$. It is observed that the for $g/L = 0.0001$ (practically zero), one recovers the values of the natural frequencies for the classical case. It is also observed that the results of Table 2 are identical to those in Papargyri-Beskou et al. [7] obtained analytically.

Table 2 First five normalized natural frequencies of a gradient elastic simply supported beam for various values of g/L

g/L	0.0001	0.005	0.010	0.050	0.100
1st	1.0000	1.00012	1.00049	1.01226	1.04819
2nd	1.0000	1.00049	1.00197	1.04819	1.18101
3rd	1.0000	1.00111	1.00443	1.10547	1.37414
4th	1.0000	1.00197	1.00786	1.18101	1.60597
5th	1.0000	1.00308	1.01226	1.27155	1.86210

Table 3 Values of υ_3' in r/s for the first three modes and various values of g/L for a gradient elastic simply supported beam

g/L	0.0001	0.005	0.010	0.050	0.100
1st	−1.0000	− 1.0000	− 1.0000	− 1.0000	− 1.0000
2nd	1.0000	1.0000	1.0000	1.0000	1.0000
3rd	−1.0000	− 1.0000	− 1.0000	− 1.0000	− 1.0000

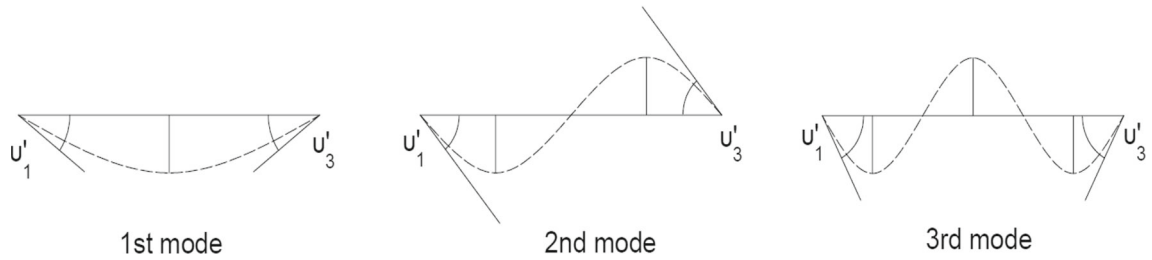

Fig. 9 Modal shapes for the first three modes of a gradient elastic simply supported beam

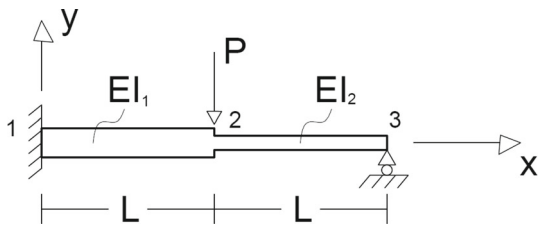

Fig. 10 Geometry and dynamic loading of a fixed-hinged gradient elastic beam composed of two members with different cross sections

Furthermore, it is also observed that the natural frequencies increase for increasing values of *g/L* as a result of the stiffening effect of gradient elasticity, exactly as in the previous example.

Once the natural (modal) frequencies ω_{n} are known, one can obtain the corresponding modal shapes from Eq. (33) by assuming $\upsilon_1'(\omega_n) = 1r/s$ and computing $\upsilon_3'(\omega_n)$ from

$$\upsilon_3'(\omega_n) = -D_{22}(\omega_n)/D_{55}(\omega_n), \tag{35}$$

Table 3 provides $\upsilon_3'$for the first three modes and various values of *g/L*, while Fig. 9 shows pictorially those results together with the complete curves of the modal shapes. It is observed that the modal shapes do not depend on g/L and hence are the same as in the classical case.

Example 3 Consider a gradient elastic beam structure composed of two members with different cross sections fixed at one end and on rollers at the other end and subjected to a vertical lateral concentrated load $P(t)$ suddenly applied at the middle of its span ($P(t) = P_0H(t)$), as shown in Fig. 10. The flexural rigidities of the two members I and II of Fig. 10 are EI_1 and EI_2, respectively, with $I_1 = 2I_2 = 2I$, while their lengths are equal to L. The geometrical and material data are the same as in Example 1. This structure is modeled by two finite elements 1–2 and 2–3 and has 3 nodes with 3 d.o.f. per node, as shown in Fig. 10. Thus, the total structural stiffness matrix resulting from the superposition of the stiffness matrices of its two elements is 9×9. The classical boundary conditions of this problem in terms of generalized nodal displacements are

$$\upsilon_1 = \upsilon_1' = \upsilon_3 = 0 \tag{36}$$

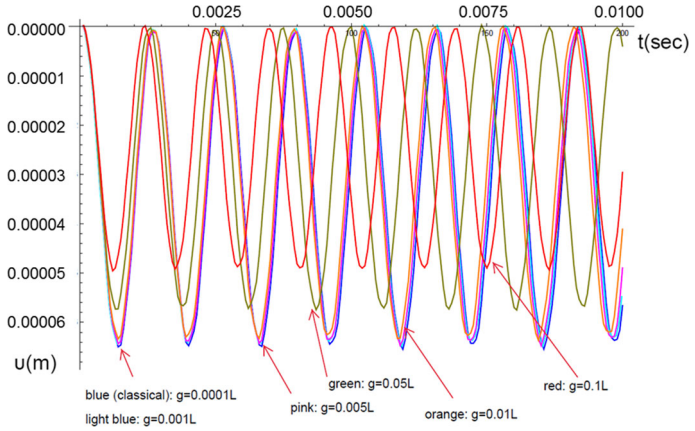

Fig. 11 Mid-span deflection for a fixed-hinged gradient elastic beam composed of two members with different cross sections for various values of *g/L* (the load is $P(t) = Po * H(t)$)

Table 4 First five natural frequencies in rad/sec of a fixed-hinged gradient elastic beam composed of two members with different cross sections for various values of g/L

g/L	0.005	0.01	0.05	0.10
1st	0.822022	0.826440	0.870422	0.947183
2nd	0.519963	0.523367	0.643586	0.815322
3rd	0.432572	0.435368	0.557716	0.739942
4th	0.382010	0.385094	0.540018	0.629935
5th	0.357994	0.360970	0.532243	0.574925

while it is assumed that there is only one non-classical boundary condition of the form

$$\upsilon_1'' = 0. \tag{37}$$

Since the applied dynamic load is a transient one, the problem will be solved with the aid of the Laplace transform, as described in Sect. 4. Thus, the response will be obtained in the Laplace-transformed domain by solving Eq. (25) with $[K(s)]$ being of the order of 5×5 (9 d.o.f. minus 4 boundary conditions) and $\{\overline{F}\}$ and $\{\overline{U}\}$ of the form

$$\begin{aligned} \{\overline{\mathrm{F}}\} &= \{-P_0/s, 0, 0, 0, 0\}^{\mathrm{T}}, \\ \{\overline{\mathrm{U}}\} &= \{\overline{v}_2, \overline{v}_2', \overline{v}_2'', \overline{v}_3', \overline{v}_3''\}^{\mathrm{T}}. \end{aligned} \tag{38}$$

Equation (25) with $\{\overline{F}\}$ and $\{\overline{U}\}$ as in (35) is solved for $\{\overline{U}\}$for a sequence of values of s, and the time domain response $\{U\}$ is obtained by a numerical inversion of the transformed solution with the aid of the algorithm of Durbin [28] as described in Sect. 4. Figure 11 depicts the history of the lateral deflection υ_2 for various values of *g/L*. It is observed that, as in previous examples, the deflection decreases for increasing values of *g/L* due to the stiffening character of gradient elasticity theory.

At this point one can approximately verify the correctness of the obtained results by recording the maximum value of υ_2(t) for the classical case ($g \to 0$) and comparing it against υ_2, i.e., its value obtained by applying the load P_0 statically. From Pegios et al. [19], one has that $\upsilon_2 = -(11/216)PL^3/\mathrm{EI}$, which for the data of this problem yields $\upsilon_2 = -0.000033090$m. On the other hand, from Fig. 11 one has for $g/L = 0.0001$ (practically zero) and the same data that the max $\upsilon_2(t) = -0.00006612 \approx 2\upsilon_2$.

This is in agreement with the fact that if the beam structure is considered approximately as a single d.o.f. system under a suddenly applied load, then the maximum value of its response is twice the value of its static response (Biggs [32]).

For the beam structure of Fig. 10 its first five natural frequencies have been also computed by solving Eq. (21) as described in Sect. 4. Table 4 provides the first five natural frequencies of the structure in rad/sec for various values of *g/L* and clearly shows their increase with increasing values of *g/L*.

6 Conclusions

On the basis of the preceding developments, one can draw the following conclusions:

(i) The dynamic stiffness matrix for a gradient elastic Bernoulli–Euler finite beam element has been constructed in the frequency domain. The element has two nodes with three degrees of freedom per node (displacement, slope, curvature).
(ii) The displacement function used is the exact solution of the governing equation of flexural beam vibrations in the frequency domain, and this results in an exact dynamic stiffness matrix, exact dynamic response to harmonically varying with time load, and exact natural frequencies.
(iii) When the external loading is transient, the response is obtained with the aid of the Laplace transform with respect to time and a numerical inversion of the transformed solution. The Laplace-transformed domain formulation is obtained from the frequency domain one by simply replacing the frequency ω by $-is$, where s is the Laplace transform parameter.
(iv) The proposed FEM formulates the problem in a static-like form in the frequency or the Laplace transform domain with obvious gains from the conceptual and practical view points. The fact that the present FEM is associated with exact stiffness matrices implies that the discretization is restricted to one finite element per physical member, which leads to matrices of much smaller size. Of course, the stiffness coefficients are more complicated than in the conventional FEM that employs approximate displacement functions in polynomial form. In general, the advantages of the proposed FEM over analytical methods for dynamic analysis of gradient elastic beam structures are generality, versatility, and efficiency, especially for complicated geometries and loading.
(v) It was observed, at least in the examples considered here, a decrease in deflections and an increase in the natural frequencies with increasing values of the gradient coefficient as a result of the stiffening effect of gradient elasticity theory.

References

1. Craighead, H.G.: Nanoelectromechanical systems. Science **290**, 1532–1535 (2000)
2. Senturia, S.D.: Microsystem Design. Kluwer Academic Publishers, Boston (2001)
3. Mindlin, R.D.: Microstructure in linear elasticity. Arch. Ration. Mech. Anal. **16**, 51–78 (1964)
4. Tsinopoulos, S.V., Polyzos, D., Beskos, D.E.: Static and dynamic BEM analysis of strain gradient elastic solids and structures. Comput. Model. Eng. Sci. (CMES) **86**, 113–144 (2012)
5. Chang, C.S., Gao, J.: Wave propagation in granular rod using high-gradient theory. J. Eng. Mech. ASCE **123**, 52–59 (1997)
6. Papargyri-Beskou, S., Tsepoura, K.G., Polyzos, D., Beskos, D.E.: Bending and stability analysis of gradient elastic beams. Int. J. Solids Struct. **40**, 385–400 (2003)
7. Papargyri-Beskou, S., Polyzos, D., Beskos, D.E.: Dynamic analysis of gradient elastic flexural beams. Struct. Eng. Mech. **15**, 705–716 (2003)
8. Lam, D.C.C., Yang, F., Chong, A.C.M., Wang, J., Tong, P.: Experiments and theory in strain gradient elasticity. J. Mech. Phys. Solids **51**, 1477–1508 (2003)
9. Giannakopoulos, A.E., Stamoulis, K.: Structural analysis of gradient elastic components. Int. J. Solids Struct. **44**, 3440–3451 (2007)
10. Kong, S., Zhou, S., Nie, Z., Wang, K.: Static and dynamic analysis of micro beams based on strain gradient elasticity theory. Int. J. Eng. Sci. **47**, 487–498 (2009)
11. Papargyri-Beskou, S., Beskos, D.E.: Static analysis of gradient elastic bars, beams, plates and shells. Open Mech. J. **4**, 65–73 (2010)
12. Papargyri-Beskou, S., Polyzos, D., Beskos, D.E.: Wave dispersion in gradient elastic solids and structures : a unified treatment. Int. J. Solids Struct. **46**, 3751–3759 (2009)
13. Wang, B., Zhao, J., Zhou, S.: A microscale Timoshenko beam model based on strain gradient elasticity theory. Eur. J. Mech. A/Solids **29**, 591–599 (2010)
14. Akgoz, B., Civalek, O.: A size-dependent shear deformation beam model based on the strain gradient elasticity theory. Int. J. Eng. Sci. **70**, 1–14 (2013)
15. Triantafyllou, A., Giannakopoulos, A.E.: Structural analysis using a dipolar elastic Timoshenko beam. Eur. J. Mech. A/Solids **39**, 218–228 (2013)
16. Martin, H.C.: Introduction to Matrix Methods of Structural Analysis. McGraw-Hill, New York (1966)
17. Artan, R., Batra, R.C.: Free vibrations of strain gradient beam by the method of initial values. Acta Mech. **223**, 2393–2409 (2012)
18. Artan, R., Toksoz, A.: Stability analysis of gradient elastic beams by the method of initial value. Arch. Appl. Mech. **83**, 1129–1144 (2013)

19. Pegios, I.P., Papargyri-Beskou, S., Beskos, D.E.: Finite element static and stability analysis of gradient elastic beam structures. Acta Mech. **226**, 745–768 (2015)
20. Asiminas E.L., Koumousis V.K.: A beam finite element based on gradient elasticity. In: Beskos, D.E., Stavroulakis, G.E. (eds.) Proceedings of 10th HSTAM International Congress on Mechanics, May 25–27, 2013, paper no 123. Technical University of Crete, Chania, Crete, Greece Press (2013)
21. Kahrobaiyan, M.H., Asghari, M., Ahmadian, M.T.: Strain gradient beam element. Finite Elem. Anal. Des. **68**, 63–75 (2013)
22. Zhang, B., He, Y., Liu, D., Gan, Z., Shen, L.: Non-classical Timoshenko beam element based on the strain gradient elasticity theory. Finite Elem. Anal. Des. **79**, 22–39 (2014)
23. Kohrobaiyan, M.H., Asghari, M., Ahmadian, M.T.: A strain gradient Timoshenko beam element: application to MEMS. Acta Mech. **226**, 505–525 (2015)
24. Bakhtiari-Nejad, F., Nazemizadeh, M.: Size-dependent dynamic modeling and vibration analysis of MEMS/NEMS-based nanomechanical beam based on the nonlocal elasticity theory. Acta Mech. **227**, 1363–1379 (2016)
25. Beskos, D.E., Narayanan, G.V.: Dynamic response of frameworks by numerical Laplace transform. Comput. Methods Appl. Mech. Eng. **37**, 289–307 (1983)
26. Mathematica, 2004, Version 11.1, Wolfram Research Inc., Champaign, Illinois, USA
27. Kitahara, M.: Boundary Integral Equation Methods in Eigenvalue Problems of Elastodynamics and Thin Plates. Elsevier, Amsterdam (1985)
28. Durbin, F.: Numerical inversion of Laplace transform : an efficient improvement of Dubner and Abate's method. Comput. J. **17**, 371–376 (1974)
29. Narayanan, G.V., Beskos, D.E.: Numerical operational methods for time- dependent linear problems. Int. J. Numer. Methods Eng. **18**, 1829–1854 (1982)
30. Beskos, D.E., Michael, A.Y.: Solution of plane transient elastodynamic problems by finite elements and Laplace transform. Comput. Struct. **18**, 695–701 (1984)
31. Rao, S.S.: Vibration of Continuous Systems. Wiley, Hoboken (2007)
32. Biggs, J.M.: Introduction to Structural Dynamics. McGraw Hill Book Co, New York (1964)